

Nature of Bosonic Excitations Revealed by High-Energy Charge Carriers

Jan Kogoj,^{1,*} Marcin Mierzejewski,² and Janez Bonča^{1,3}

¹*J. Stefan Institute, 1000 Ljubljana, Slovenia*

²*Institute of Physics, University of Silesia, 40-007 Katowice, Poland*

³*Faculty of Mathematics and Physics, University of Ljubljana, 1000 Ljubljana, Slovenia*

(Received 21 June 2016; published 23 November 2016)

We address a long-standing problem concerning the origin of bosonic excitations that strongly interact with charge carriers. We show that the time-resolved pump-probe experiments are capable of distinguishing between regular bosonic degrees of freedom, e.g., phonons, and the hard-core bosons, e.g., magnons. The ability of phonon degrees of freedom to absorb essentially an unlimited amount of energy renders relaxation dynamics nearly independent of the absorbed energy or fluence. In contrast, the hard core effects pose limits on the density of energy stored in the bosonic subsystems resulting in a substantial dependence of the relaxation time on the fluence and/or excitation energy. Very similar effects can be observed also in a different setup when the system is driven by multiple pulses.

DOI: 10.1103/PhysRevLett.117.227002

Solids are complex objects with different degrees of freedom; hence, the charge carriers are simultaneously coupled to various types of bosonic excitations like phonons, magnons, plasmons, or others. The long-standing problem in the studies on strongly correlated systems is to single out the strongest, and thus probably the most relevant interaction. However, for many important materials, including the unconventional superconductors, we are still seeking the answer to a more modest question, whether the strongest coupling of charge carriers is to phonons or to some kind of magnetic excitations. The essential qualitative difference between these excitations is that the latter ones are hard-core (HC) quasiparticles; i.e., their spatial density is typically limited by one boson per lattice site. It is rather clear that the HC effects become important first in the vicinity of this bound, i.e., when the energy density is of the order of the frequency of the bosonic excitations. However, it might be impossible to heat up the entire system to such high energies since, e.g., the corresponding temperature may be too close to the melting point. A very promising solution is to excite only targeted degrees of freedom.

This solution is utilized in the recent time resolved photoemission and optical spectroscopies, where one studies ultrafast relaxation of a few highly excited charge carriers [1–9]. These carriers lower high initial kinetic energy (of the order of 1–2 eV) in a narrow time window by emitting many of most strongly coupled bosons. In the vicinity of the excited charge carriers, the concentration of emitted bosons may be high enough so that the HC effects become visible.

In the majority of the recent theoretical papers, the ultrafast relaxation of highly excited carriers has been discussed separately for the couplings to phonons [10–24] and to the magnetic excitations [25–28]. On the one hand, the electron-phonon coupling is usually

described within the Holstein model by two independent parameters: the dimensionless coupling strength λ and the phonon frequency ω . The electron-phonon interaction is efficient in any dimension; hence it has been mostly studied in the simplest case of the one-dimensional (1D) systems. On the other hand, the coupling to the magnetic excitations is studied mainly within the Hubbard or the t - J models. Each of the latter models contains a single free parameter (U/t or J/t) which encodes the coupling strength as well as the frequency of the excitations. Since the spin and the charge degrees of freedom are separated in the 1D systems, relaxation due to magnetic excitations should be studied at least in two dimensions. Because of the essential differences between the studied models, it is difficult to identify the distinctive qualitative features of both mechanisms. In the present work we fill this important gap. We compare the relaxation of charge carriers in two models, chosen such that all the emerging differences are solely due to HC effects of the bosonic excitations. We show that if the relaxation is due to the coupling to HC bosons, then the relaxation time shows pronounced dependence on the excitation energy and/or the density of excited carriers. The opposite holds true for coupling to standard bosonic degrees of freedom.

Model.— We consider two models on a one-dimensional ring with L sites, each containing a single electron. The first one is the Holstein model (HM) while the second is a HC boson model (HCM) where phonon degrees of freedom are replaced by hard core bosons. Hamiltonians of both models have a very similar structure:

$$H_{\text{sys}} = H_{\text{kin}} + H_{\text{bos}} + H_{\text{int}}, \quad (1)$$

where individual parts of H_{sys} are as follows:

$$H_{\text{kin}} = -t_0 \sum_j (e^{i\phi(t)} c_j^\dagger c_{j+1} + \text{H.c.}),$$

$$H_{\text{bos}} = \omega \sum_j b_j^\dagger b_j, \quad (2)$$

$$H_{\text{int}} = -g \sum_j c_j^\dagger c_j (b_j^\dagger + b_j), \quad (3)$$

where t_0 is the hopping amplitude, c_j is a fermion annihilation operator on site j , and b_j represents either the phonon or HC boson. There is at most one HC boson per site; hence $b_i^\dagger b_i^\dagger = 0$. This restriction shows up in specific commutation relations $[b_i, b_j^\dagger] = \delta_{ij}(1 - 2b_i^\dagger b_i)$ for the latter operators. For clarity of comparison we introduce identical dispersionless frequency ω and coupling g for phonons and HC bosons alike. The $\phi(t)$ represents the phase gained by the electron as it hops between successive sites. It is used to pump energy into the system as described in the last part of this work. We measure time in units \hbar/t_0 and set $\hbar = 1$.

We solve both models using the Lanczos-based diagonalization defined within a limited functional space (LFS) to obtain the ground state as well as for the time evolution. The generation of the LFS efficiently selects states with different phonon configurations in the vicinity of the electron thus enabling numerically an exact solution of the polaron problem at zero temperature [29,30], and it is well suited also to describe polaron systems far from the equilibrium [10,21,31,32]. A detailed description of this numerical approach can be found in Ref. [31].

In the first part of this work we start the time evolution from the free electron wave function at a given wave number k , $|\psi_0(t=0)\rangle = c_k^\dagger |0\rangle$ where $|0\rangle$ represents vacuum state for electrons and bosons. We choose the initial kinetic energy of the electron $E_{\text{kin}}(t=0) = -2t_0 \cos(k)$ to be much larger than the ground-state $E_{\text{kin}}^{\text{GS}}$ of the polaron. We then perform the time evolution under H_{sys} , Eq. (1), to obtain the wave function $|\psi(t)\rangle$ of the system. This approach simulates polaron formation starting from a free electron with variable (possibly very high) initial kinetic energy.

In Fig. 1(a) we present a comparison of $E_{\text{kin}}(t) = \langle H_{\text{kin}}(t) \rangle$ of HM and HCM for different values of initial k . In all cases we observe a decrease of $E_{\text{kin}}(t)$ towards quasisteady state values \bar{E}_{kin} that remain consistently above their respective ground-state values $E_{\text{kin}}^{\text{GS}}$. We should stress that the total energy of the system E_{sys} remains constant during the time evolution and it equals the initial value of the kinetic energy, i.e., $E_{\text{sys}} = E_{\text{kin}}(t=0)$. The decrease of $E_{\text{kin}}(t)$ is thus intimately connected to the increase of the phonon or HC boson energy. The main difference between the models under consideration is that phonon degrees of freedom can absorb in principle an infinite amount of energy while HC bosons can absorb at most ω of energy per site. For small k , i.e., $k = \pi/2$ and $5\pi/8$, relaxation dynamics of HM and HCM are nearly indistinguishable.

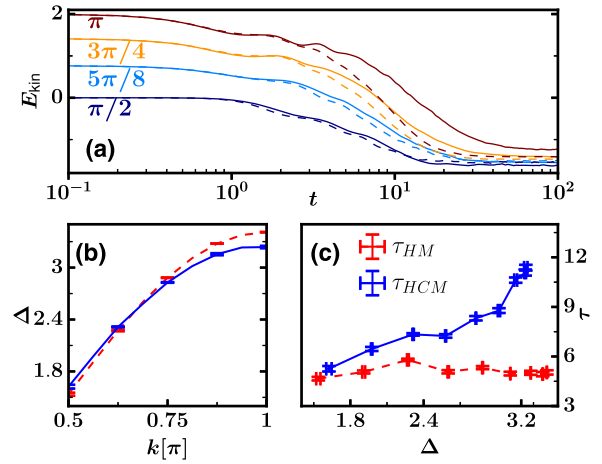


FIG. 1. (a) $E_{\text{kin}}(t)$ vs time t for different values of k . Dashed (full) lines represent results for HM (HCM). Other parameters of the Hamiltonian in Eq. (2) are $\omega = 0.5$, $g = \sqrt{0.5}$ and the size of the system with periodic boundary conditions is $L = 16$. Unless otherwise specified, identical parameters were used in all subsequent figures. The phase is set to $\phi(t) = 0$ in all figures except in Fig. 3. (b) Dependence of Δ on the wave number k of the initial free electron wave function. (c) Relaxation time τ_{HM} (τ_{HCM}) for HM (HCM) vs excitation energy Δ , extracted from data presented in (a) using the following analytical form $E_{\text{kin}}(t) = a \exp(-\sqrt{(t/\tau)^2 + b^2} + b) + c$; for details of fitting see also Refs. [33,34]. Error bars in (b) and (c) correspond to threefold standard deviation. Errors in specifying Δ are due to small time fluctuation of $E_{\text{kin}}(t)$ in the long-time limit.

For larger values of $k \geq 3\pi/4$, however, relaxation of the HM seems to be substantially faster than that of the HCM.

In Fig. 1(c) we present the central result of this work, that is, the comparison of relaxation times τ_{HM} and τ_{HCM} of the HM and HCM, respectively, as a function of the excitation energy that is defined as a difference between the initial kinetic energy of the electron and the average kinetic energy in the quasisteady state: $\Delta = E_{\text{kin}}(t=0) - \bar{E}_{\text{kin}}$. We found a relatively weak dependence of relaxation times τ_{HM} on Δ ; in particular, there is no abrupt raise of τ_{HM} at large values of Δ . In contrast, much more pronounced dependence on Δ is found in the case of τ_{HCM} . We observe a sharp up-turn of τ_{HCM} for larger values of Δ signaling a significant slowing down of the relaxation process in the HCM. In contrast, at small $\Delta \sim 1.5$, τ_{HCM} approaches τ_{HM} . The dependence of Δ on the wave vector k is presented in Fig. 1(b).

To gain a deeper understanding of the different relaxation processes in models under the investigation, we computed the average number of bosonic excitations per site, given by $n_{\text{bos}} = \langle \psi(t) | \sum_i b_i^\dagger b_i | \psi(t) \rangle / L$. We first note that there is no upper bound on n_{bos} in the HM case. In contrast, there is a formal upper bound $n_{\text{bos}} \leq 1$ in the HCM while already twice smaller concentration $n_{\text{bos}} = 0.5$ is reached in the limit of infinite temperature. As it is shown in Fig. 2(a), n_{bos} in the HM keeps increasing with increasing k , whereas we observe signs of saturation in the HCM case

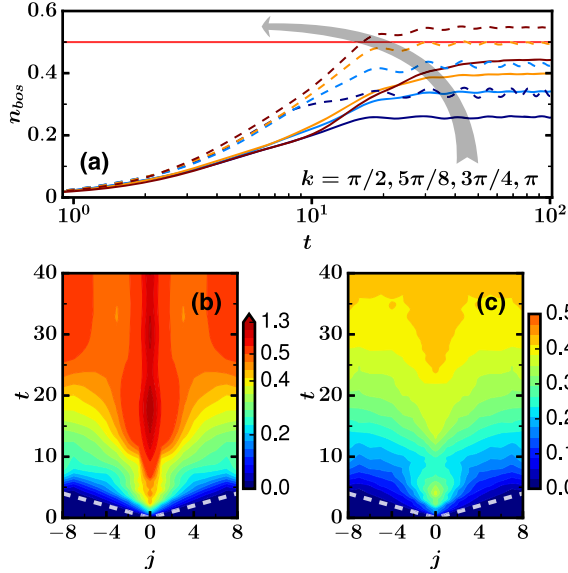


FIG. 2. (a) Average number of bosonic excitations per site n_{bos} vs t for different values of k corresponding to different Δ as depicted in Fig. 2(b). Dashed (full) lines represent results for the HM (HCM). The horizontal line indicates the infinite-temperature value of n_{bos} in the HCM. (b),(c) Spread of bosonic excitations $\gamma(j, t)$ for the HM and HCM, respectively, for $k = \pi$. Dashed white lines represent the Lieb-Robinson bound as described in the text. To facilitate a straightforward comparison between models, identical color coding was used in both panels.

as n_{bos} moves closer to its infinite-temperature value $n_{\text{bos}} = 0.5$ at maximal excitation energy reached at $k = \pi$.

In order to estimate the density of magnetic excitations in the existing pump-probe experiments, we follow Ref. [9]. It was reported that the pump pulse with the fluence $700 \mu\text{J}/\text{cm}^2$ excites in cuprates approximately one charge carrier with energy 2.5 eV per 100 Cu atoms. Taking the relevant exchange interaction $J = 0.11$ eV and the ground state energy of the two-dimensional Heisenberg model -0.67 J/site [35] one finds that heating the magnetic subsystem from zero to infinite temperature requires the energy density 0.07 eV/site which is roughly three times larger than applied in Ref. [9].

However, the HC effects may become important already for $n_{\text{bos}} \ll 1/2$ when the concentration of bosons is high only locally, in the vicinity of the charge carrier. In order to study such scenario, we present in Figs. 2(b) and 2(c) surface plots of the correlation function

$$\gamma(j, t) = \langle \psi(t) | \sum_i c_i^\dagger c_i b_{i+j}^\dagger b_{i+j} | \psi(t) \rangle. \quad (4)$$

$\gamma(j, t)$ enables us to follow the spread of bosonic degrees of freedom during the time evolution. At short times, $t \lesssim 5$ and small intensities, $\gamma(j, t) \lesssim 0.1$, we observe a similar spread of the front of bosonic excitations away from the electron position at $j = 0$. This spread is given by the Lieb-Robinson's velocity (i.e., the maximal speed at which information propagates) that in both models equals the

maximal velocity of a free electron $v_{\text{LR}} = 2t_0$. Since bosons of both types are dispersionless, the observed velocity is due to the electron that moves away from the bosonic excitation. At later times and larger intensities we observe a qualitative difference in $\gamma(j, t)$ between both models. In the HM there is an excess of extra phonon excitations at and in the close proximity of the electron's position. In contrast, the HCM case bosonic degrees of freedom spread much more uniformly throughout the entire system. This represents the main mechanism that causes substantial slowing down of relaxation in HCM at larger values of Δ . As Δ increases far beyond the typical bosonic frequency, $\Delta \gtrsim \omega_0$, in a semi-classical picture, the charge has to travel ever larger distance to dispose of the excess energy.

We have demonstrated that the HC effects slow down the relaxation of highly excited charge carriers. Therefore, the future experiments showing the relaxation time vs the excitation energy may shed light on the type of bosons, which are most strongly coupled to the carriers. However, in the majority of the experimental setups it is easy to tune the density of photoexcited carriers (e.g., by changing the fluence) but not necessarily their energy. Direct numerical simulations of the former problem cannot be carried out within the present model with a single charge carrier. However, we expect that a qualitatively similar picture may be obtained from the studies of a slightly different experimental setup when a charge carrier is driven by multiple pulses. The discussed scenario should hold independently of whether the bosons are excited by a single or various charge carriers. At the end, what matters for the hard-core effects is the density of the bosons and not their source.

In Fig. 3(a) we show how the relaxation changes upon applying subsequent pulses to HM and HCM. We have

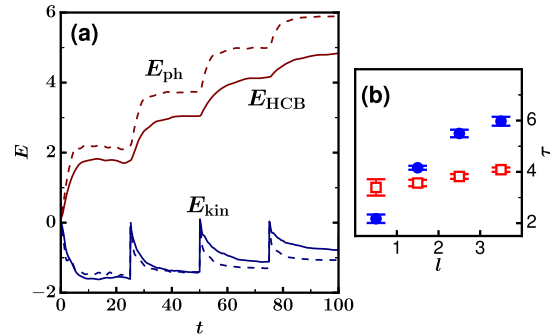


FIG. 3. Kinetic energy E_{kin} , phonon energy E_{ph} and hard core boson energy E_{HCB} vs time in (a). Dashed (full) lines represent results for the HM (HCM). $\omega = g = 0.75$, and $L = 16$ was used in this particular case. Note that the upper limit of E_{HCB} , reached at infinite temperature, is $E_{\text{HCB}}^{\text{max}} = L\omega/2 = 6$. Multiple spikes in E_{kin} are due to steplike jumps in the phase $\phi(t) = \pi/2 \sum_{i=0}^3 \theta(t - i\Delta t)$ where $\Delta t = 25$ and $\theta(x)$ is the Heaviside step function. In (b) we present relaxation time τ with squares (full circles) for the HM (HCM), extracted from the relaxation of $E_{\text{kin}}(t)$ in distinct time intervals between successive steplike changes of $\phi(t)$.

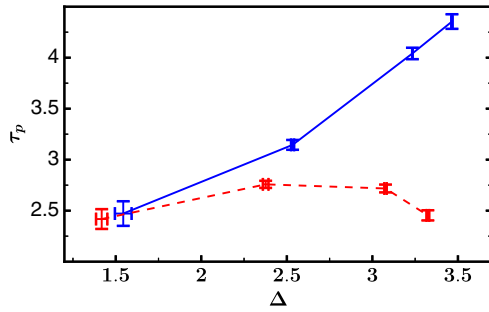


FIG. 4. Primary relaxation times τ_p of a generalized model containing both phonon as well as HC boson degrees of freedom with identical frequencies $\omega_{\text{phon}} = \omega_{\text{HCbos}} = 0.5$, respectively, but different coupling constants: $\lambda_{\text{HCbos}} = g_{\text{HCbos}}^2/2\omega t_0 = 0.5$ and $\lambda_{\text{phon}} = g_{\text{phon}}^2/2\omega t_0 = 0.1$ (full line) and $\lambda_{\text{HCbos}} = 0.1$ and $\lambda_{\text{phon}} = 0.5$ (dashed line). Smaller system with $L = 12$ sites has been used in this case.

simulated this case by starting the time evolution from the polaron ground state wave function at $t = 0^-$, followed by successive steplike jumps in the phase $\phi(t)$ as described in the caption of Fig. 3. Each jump in $\phi(t)$ causes an abrupt jump of E_{kin} followed by a relaxation process in which a decrease in E_{kin} is followed by the increase of the corresponding boson energy. In the HCM, the relaxation after succeeding pulses becomes visibly slower as the density of excited hard-core bosons becomes comparable with its value at infinite temperature, i.e., $E_{\text{HCM}}^{\text{max}}/L = \omega/2$; see also the caption in Fig. 3. In contrast, relaxation in the HM does not show any substantial dependence on the number of preceding pulses. This is clearly seen in Fig. 3(b) where we present relaxation times for both models as extracted from the fitting procedure as described in Ref. [33] in distinct time intervals.

To test whether the distinction between phonon and HC boson degrees of freedom is possible in a more realistic situation, we have investigated relaxation dynamics of a generalized Holstein-HC-boson model where a single electron is concurrently coupled to phonon and HC boson degrees of freedom. In such case one finds two relaxation times [33] that may differ by several orders of magnitude [4]. Here we focus on the shortest one, denoted as the primary relaxation time τ_p , shown in Fig. 4. In the case when coupling to HC boson degrees of freedom is dominant, we observe a strong increase of τ_p with increasing Δ , while τ_p remains weakly dependent on Δ when coupling to phonon degrees of freedom is dominant. Results on the generalized Holstein-HC model demonstrate that when the primary relaxation is dominated by a single bosonic excitation, the fluence dependence of the primary relaxation time brings to light whether this particular mode represents standard bosons or hard-core particles.

Summary.— We propose a simple mechanism to distinguish between two different classes of bosonic excitations that are responsible for the primary (fastest) relaxation

mechanism of a photo-excited charge carrier in time-resolved pump-probe experiments. The proposed mechanism is based on the recognition that phonon degrees of freedom can absorb essentially an unlimited amount of energy while in contrast, the hard core effects, typical for, e.g., magnon excitations, pose strict limits on the density of absorbed energy. For this reason the relaxation dynamics of the charge carrier coupled to phonon degrees of freedom very weakly depends on the excitation energy, while the opposite is true when the charge carrier is coupled to HC boson excitations. In the latter case the relaxation becomes less effective when the absorbed energy approaches the typical HC boson frequency, i.e., $\Delta \sim \omega$. The density of excited bosons can be tuned either by changing the fluence of a single pump pulse or by driving the system by multiple pulses. In the latter case the time span between the first and the last pulses should be significantly smaller than the secondary relaxation time when other, weakly coupled degrees of freedom start to influence the relaxation process.

To gain a clear distinction between the two different cases, we performed simulations on nearly identical models containing either Einstein phonons or dispersionless HC bosons. However, in more realistic systems dispersionless HC bosons should be replaced by, e.g., dispersive magnetic excitations with a given magnon velocity v_{mag} . Still, even in this case the slowing down of relaxation due to HC effects is expected in two spacial dimensions when $\Delta \sim \omega(v_{\text{mag}}\tau)^2$. To the best of our best knowledge, the predictions of this work have not been yet tested experimentally. However, the very recent experiments on cuprates show significant fluence dependence of the relaxation times (see Fig. 5 in Ref. [8]). The HC effects should be important for the relaxation of states far above the Fermi energy, when the excitation energies are larger than the boson frequency. Contrary to this, the relaxation of states in the vicinity of the Fermi energy may be quite different. It should not be affected by the HC effects and may involve different bosonic excitations [8].

We acknowledge stimulating discussions with U. Bowensiepen and C. Giannetti. J. B. acknowledges discussions with A. Polkovnikov and M. Rigol as well as support by the P1-0044 of ARRS, Slovenia. M. M. acknowledges support from the DEC-2013/11/B/ST3/00824 project of the National Science Centre, Poland. J. K. acknowledges financial assistance by the Alexander von Humboldt Foundation. This work was performed, in part, at the Center for Integrated Nanotechnologies, a U.S. Department of Energy, Office of Basic Energy Sciences user facility.

*Corresponding author.
Janez.Bonca@ijs.si

[1] H. Okamoto, T. Miyagoe, K. Kobayashi, H. Uemura, H. Nishioka, H. Matsuzaki, A. Sawa, and Y. Tokura, Ultrafast charge dynamics in photoexcited Nd_2CuO_4 and La_2CuO_4

- cuprate compounds investigated by femtosecond absorption spectroscopy, *Phys. Rev. B* **82**, 060513 (2010).
- [2] C. Gadermaier, A. S. Alexandrov, V. V. Kabanov, P. Kusar, T. Mertelj, X. Yao, C. Manzoni, D. Brida, G. Cerullo, and D. Mihailovic, Electron-Phonon Coupling in High-Temperature Cuprate Superconductors Determined from Electron Relaxation Rates, *Phys. Rev. Lett.* **105**, 257001 (2010).
- [3] R. Cortés, L. Rettig, Y. Yoshida, H. Eisaki, M. Wolf, and U. Bovensiepen, Momentum-Resolved Ultrafast Electron Dynamics in Superconducting $\text{Bi}_2\text{Sr}_2\text{CaCu}_2\text{O}_{8+\delta}$, *Phys. Rev. Lett.* **107**, 097002 (2011).
- [4] S. Dal Conte *et al.*, Disentangling the electronic and phononic glue in a high- T_c superconductor, *Science* **335**, 1600 (2012).
- [5] C. Gadermaier *et al.*, Strain-Induced Enhancement of the Electron Energy Relaxation in Strongly Correlated Superconductors, *Phys. Rev. X* **4**, 011056 (2014).
- [6] F. Novelli *et al.*, Witnessing the formation and relaxation of dressed quasi-particles in a strongly correlated electron system, *Nat. Commun.* **5**, 5112 (2014).
- [7] J. D. Rameau *et al.*, Photoinduced changes in the cuprate electronic structure revealed by femtosecond time- and angle-resolved photoemission, *Phys. Rev. B* **89**, 115115 (2014).
- [8] J. D. Rameau *et al.*, Time-resolved boson emission in the excitation spectrum of $\text{Bi}_2\text{Sr}_2\text{CaCu}_2\text{O}_{8+\delta}$, [arXiv:1505.07055](https://arxiv.org/abs/1505.07055).
- [9] S. Dal Conte *et al.*, Snapshots of the retarded interaction of charge carriers with ultrafast fluctuations in cuprates, *Nat. Phys.* **11**, 421 (2015).
- [10] D. Golež, J. Bonča, L. Vidmar, and S. A. Trugman, Relaxation Dynamics of the Holstein Polaron, *Phys. Rev. Lett.* **109**, 236402 (2012).
- [11] G. De Filippis, V. Cataudella, E. A. Nowadnick, T. P. Devereaux, A. S. Mishchenko, and N. Nagaosa, Quantum Dynamics of the Hubbard-Holstein Model in Equilibrium and Nonequilibrium: Application to Pump-Probe Phenomena, *Phys. Rev. Lett.* **109**, 176402 (2012).
- [12] H. Matsueda, S. Sota, T. Tohyama, and S. Maekawa, Relaxation dynamics of photocarriers in one-dimensional Mott insulators coupled to phonons, *J. Phys. Soc. Jpn.* **81**, 013701 (2012).
- [13] D. M. Kennes and V. Meden, Relaxation dynamics of an exactly solvable electron-phonon model, *Phys. Rev. B* **82**, 085109 (2010).
- [14] A. F. Kemper, M. Sentef, B. Moritz, C. C. Kao, Z. X. Shen, J. K. Freericks, and T. P. Devereaux, Mapping of unoccupied states and relevant bosonic modes via the time-dependent momentum distribution, *Phys. Rev. B* **87**, 235139 (2013).
- [15] M. Sentef, A. F. Kemper, B. Moritz, J. K. Freericks, Z.-X. Shen, and T. P. Devereaux, Examining Electron-Boson Coupling Using Time-Resolved Spectroscopy, *Phys. Rev. X* **3**, 041033 (2013).
- [16] P. Werner and M. Eckstein, Phonon-enhanced relaxation and excitation in the Holstein-Hubbard model, *Phys. Rev. B* **88**, 165108 (2013).
- [17] V. V. Baranov and V. V. Kabanov, Theory of electronic relaxation in a metal excited by an ultrashort optical pump, *Phys. Rev. B* **89**, 125102 (2014).
- [18] A. F. Kemper, M. A. Sentef, B. Moritz, J. K. Freericks, and T. P. Devereaux, Effect of dynamical spectral weight redistribution on effective interactions in time-resolved spectroscopy, *Phys. Rev. B* **90**, 075126 (2014).
- [19] P. Werner and M. Eckstein, Field-induced polaron formation in the Holstein-Hubbard model, *Europhys. Lett.* **109**, 37002 (2015).
- [20] Y. Murakami, P. Werner, N. Tsuji, and H. Aoki, Interaction quench in the Holstein model: Thermalization crossover from electron- to phonon-dominated relaxation, *Phys. Rev. B* **91**, 045128 (2015).
- [21] F. Dorfner, L. Vidmar, C. Brockt, E. Jeckelmann, and F. Heidrich-Meisner, Real-time decay of a highly excited charge carrier in the one-dimensional Holstein model, *Phys. Rev. B* **91**, 104302 (2015).
- [22] S. Sayyad and M. Eckstein, Coexistence of excited polarons and metastable delocalized states in photoinduced metals, *Phys. Rev. B* **91**, 104301 (2015).
- [23] A. S. Mishchenko, N. Nagaosa, G. De Filippis, A. de Candia, and V. Cataudella, Mobility of Holstein Polaron at Finite Temperature: An Unbiased Approach, *Phys. Rev. Lett.* **114**, 146401 (2015).
- [24] V. Rizzi, T. N. Todorov, J. J. Kohanoff, and A. A. Correa, Electron-phonon thermalization in a scalable method for real-time quantum dynamics, *Phys. Rev. B* **93**, 024306 (2016).
- [25] D. Golež, J. Bonča, M. Mierzejewski, and L. Vidmar, Mechanism of ultrafast relaxation of a photo-carrier in antiferromagnetic spin background, *Phys. Rev. B* **89**, 165118 (2014).
- [26] E. Iyoda and S. Ishihara, Transient carrier dynamics in a Mott insulator with antiferromagnetic order, *Phys. Rev. B* **89**, 125126 (2014).
- [27] M. Eckstein and P. Werner, Ultra-fast photo-carrier relaxation in mott insulators with short-range spin correlations, *Sci. Rep.* **6**, 21235 (2016).
- [28] D. Golež, M. Eckstein, and P. Werner, Dynamics of screening in photodoped mott insulators, *Phys. Rev. B* **92**, 195123 (2015).
- [29] J. Bonča, S. A. Trugman, and I. Batistić, Holstein polaron, *Phys. Rev. B* **60**, 1633 (1999).
- [30] L.-C. Ku, S. A. Trugman, and J. Bonča, Dimensionality effects on the Holstein polaron, *Phys. Rev. B* **65**, 174306 (2002).
- [31] L. Vidmar, J. Bonča, M. Mierzejewski, P. Prelovšek, and S. A. Trugman, Nonequilibrium dynamics of the Holstein polaron driven by an external electric field, *Phys. Rev. B* **83**, 134301 (2011).
- [32] D. Golež, J. Bonča, and L. Vidmar, Dissociation of a Hubbard-Holstein bipolaron driven away from equilibrium by a constant electric field, *Phys. Rev. B* **85**, 144304 (2012).
- [33] See the Supplemental Material at <http://link.aps.org/supplemental/10.1103/PhysRevLett.117.227002> for the dynamics in the generalized Holstein-HC-boson model and technical details concerning the extraction of the relaxation times and finite-size scaling.
- [34] S. A. Hamerla and G. S. Uhrig, Interaction quenches in the two-dimensional fermionic hubbard model, *Phys. Rev. B* **89**, 104301 (2014).
- [35] D. C. Mattis and C. Y. Pan, Ground-State Energy of Heisenberg Antiferromagnet for Spins $s = \frac{1}{2}$ and $s = 1$ in $d = 1$ and 2 Dimensions, *Phys. Rev. Lett.* **61**, 463 (1988).